

# Gas-Phase Generation, Structure, Spectroscopy, and Quantum Chemical Calculations of Fluorocarbonylsulfur Thiocyanate, FC(O)SSCN

Shengrui Tong,<sup>[a,b]</sup> Lin Du,<sup>[a,b]</sup> Li Yao,<sup>[a,b]</sup> Maofa Ge,<sup>\*,[a]</sup> and Carlos O. Della Védova<sup>[c]</sup>

**Keywords:** Structures / Ionization and dissociation processes / Photoelectron spectroscopy / Theoretical calculations

Fluorocarbonylsulfur thiocyanate, FC(O)SSCN, was generated in the gas phase from a gas–solid reaction of FC(O)SCl on the surface of finely powdered AgSCN. The reaction products were detected and characterized in situ by photoelectron spectroscopy (PES) and photoionization mass spectrometry (PIMS). The geometrical and electronic structures of FC(O)SSCN were investigated by a combination of PES and PIMS experiments, and theoretical calculations. The title compound prefers a *gauche* conformation with the C=O groups *syn* to the S–S bond; the structure of the CSSC moiety is characterized by a dihedral angle  $\delta_{\text{CSSC}} = 89.5^\circ$  and a bond length  $r_{\text{SS}} = 2.071 \text{ \AA}$  [at the B3LYP/6-311+G(3df) level] re-

sulting from the sulfur–sulfur lone-pair interactions. After ionization the ground cationic-radical form of FC(O)SSCN<sup>+</sup> adopts a *trans*-planar structure ( $\delta_{\text{CSSC}} = 180^\circ$ ) with  $C_s$  symmetry. The outermost electrons of FC(O)SSCN reside in the lone pair of the sulfur atom bonded to the C≡N group and the  $\pi$ -bond between the C and N atoms, and the experimental first vertical ionization energy of FC(O)SSCN is 10.89 eV. The possible ionization and dissociation processes of FC(O)SSCN are also discussed.

(© Wiley-VCH Verlag GmbH & Co. KGaA, 69451 Weinheim, Germany, 2008)

## Introduction

Sulfenyl-carbonyl compounds are an interesting family of molecules related to important biological systems such as coenzyme A (CoA). Their properties in the ground and excited electronic states are related to their planar structures and to the *syn*–*anti* conformational equilibrium in the gas and liquid phase. FC(O)SCl was the first example in this series that shows a photolytic interconversion process.<sup>[1]</sup> Thioester compounds containing carbonyl groups have been the subject of many theoretical and experimental investigations. Thus, a wide series of these –C(O)S-containing molecules were analyzed in order to systematically describe their conformational properties.<sup>[2]</sup>

Disulfides play an important role in living organisms. In the formation of the tertiary structure of proteins, covalent disulfide bonds are known to ensure the formation of cross-links, which are much stronger than hydrophobic interactions and hydrogen bonds.<sup>[3]</sup> The biochemical importance

of the disulfide bond is also determined by the uniqueness of the nature of the thiol-disulfide system, in which the S–S bond can be formed under conditions appropriate for biological processes. Because of the frequency of disulfide bridges in the structure of many proteins, enzymes, and antibiotics, this bond plays an important role in stabilizing the structure and in determining the biological activity of the molecules.<sup>[4–8]</sup> Recently, considerable attention has been paid to the structural and conformational preferences of simple disulfides.<sup>[5–7,9–11]</sup> Geometric gas-phase structures of noncyclic disulfides XSSX are characterized by a *gauche* conformation around the S–S bond. Structural studies of nonsymmetrically substituted disulfides of the XSSY type are less common. Recently, gas electron diffraction (GED) or microwave spectroscopy studies on the structures of FC(O)SSCF<sub>3</sub>, FC(O)SSCH<sub>3</sub>, and FC(O)SSC(O)CF<sub>3</sub> have been performed in the gas phase.<sup>[5–7]</sup> Experimental and theoretical studies on substituted disulfides are of great importance because results from these studies can provide a sound basis for unravelling the complexity of sulfur–sulfur bonding interactions.<sup>[2,10]</sup>

Thiocyanates with an SCN group attached directly to the sulfur atom, XSSCN, which possess a sulfur–sulfur bond, have long been known. The first unstable thiocyanate containing a single S–S bond, NCSSCN, was synthesized by Söderbäck in 1918.<sup>[8]</sup> Various polysulfides NCS<sub>n</sub>CN ( $n < 9$ ) have been studied by Raman spectroscopy.<sup>[12]</sup> Thiazyl thiocyanide, NSSCN, was generated by an on-line process using NSCl passed over heated AgSCN and studied by gas-phase FTIR spectroscopy.<sup>[9]</sup>

[a] Beijing National Laboratory for Molecular Sciences (BNLMS), State Key Laboratory for Structural Chemistry of Unstable and Stable Species, Institute of Chemistry, Chinese Academy of Sciences, 100190 Beijing, P. R. China  
Fax: +86-10-62554518  
E-mail: gemaofa@iccas.ac.cn

[b] Graduate University of Chinese Academy of Sciences, 100039 Beijing, P. R. China

[c] CEQUINOR (UNLP-CONICET) and Laboratorio de Servicios a la Industria y al Sistema Científico (UNLP-CIC-CONICET), Departamento de Química, Facultad de Ciencias Exactas, Universidad Nacional de La Plata, 47 esq. 115, 1900 La Plata, Argentina

Fluorocarbonylsulfur thiocyanate, FC(O)SSCN, was first synthesized by Haas and Reinke and was characterized by IR and  $^{19}\text{F}$  NMR spectroscopy.<sup>[13,14]</sup> There is no photoelectron spectroscopy (PES) study on the electronic structure of this molecule. In this work, we report on a combined experimental and theoretical investigation of FC(O)SSCN. Quantum chemical calculations were performed in order to study the structural properties of the title compound, together with the cationic-radical form,  $[\text{FC}(\text{O})\text{SSCN}^+]$ , in its ground state. The electronic structure of the neutral compound was investigated by means of photoelectron spectroscopy. Photoionization mass spectrometry (PIMS) was used to gather more information about ionization and dissociation processes of FC(O)SSCN. The first vertical ionization energy and the mass spectrum of FC(O)SSCN were determined by PES and PIMS, respectively, for the first time.

## Results and Discussion

### Molecular Structure

The conformation of disulfides is mainly determined by the geometry of the SS moieties. Gas-phase structures of noncyclic disulfides  $\text{XSSY}$  are characterized by dihedral angles  $\delta_{\text{XSSY}}$  close to  $90^\circ$ . HSSH, the parent compound of the  $\text{XSSY}$  disulfanes, has a dihedral angle of  $90.76^\circ/90.34^\circ$ .<sup>[15,16]</sup> Because the S–S bond length is larger than the O–O bond length, the steric repulsion between the substituents is reduced in disulfides. According to the results of experiments, the most stable conformer of the FC(O)SSCH<sub>3</sub> molecule adopts a *gauche* conformation, characterized by a dihedral angle  $\delta_{\text{CSSC}} = 83.5^\circ$ .<sup>[6]</sup> Similar phenomena were found in CH<sub>3</sub>OC(O)SSCN,<sup>[10]</sup> CH<sub>3</sub>C(O)-OSSOC(O)CH<sub>3</sub>,<sup>[17]</sup> and ClSSCN.<sup>[18]</sup> So the starting geometry of the *gauche* conformer of FC(O)SSCN for quantum chemical calculations was based on the structure of the *gauche* conformer of FC(O)SSCH<sub>3</sub> as measured by gas electron diffraction (GED). The optimized geometry of FC(O)SSCN is shown in Figure 1 [*gauche* (sp)].

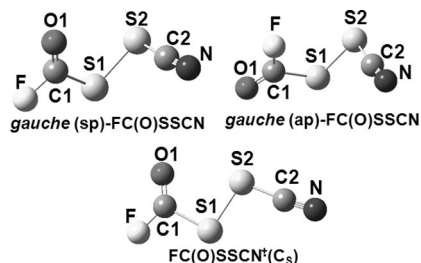


Figure 1. Schematic representation of the two stable conformers of FC(O)SSCN.

In order to search for other possible conformers with different  $\delta_{\text{CSSC}}$  angles relaxed scans of the potential energy surface were performed by rotating the torsional dihedral angle  $\delta_{\text{CSSC}}$  in steps of  $10^\circ$  ranging from  $0$  to  $360^\circ$  at the HF/6-31G(d), B3LYP/6-31G(d), and MP2/6-31G(d) levels (Figure 2). There is no other minimum except the expected

minima for the identified *gauche* structures, which exhibit a dihedral angle around  $80^\circ$  [MP2/6-31G(d) result],  $90^\circ$  [B3LYP/6-31G(d) and HF/6-31G(d) results],  $280^\circ$  [MP2/6-31G(d) result], or  $270^\circ$  [B3LYP/6-31G(d) and HF/6-31G(d) results]. The energy barrier for the S–S rotation is 3.83, 5.00, and 4.62 kcal/mol at the B3LYP/6-31G(d), MP2/6-31G(d), and HF/6-31G(d) levels, respectively. This behavior is due to the S–S lone-pair repulsion and steric interactions between FC(O) and CN moieties, which is similar to FC(O)SSCH<sub>3</sub> and CH<sub>3</sub>OC(O)SSCN.<sup>[6,10]</sup>

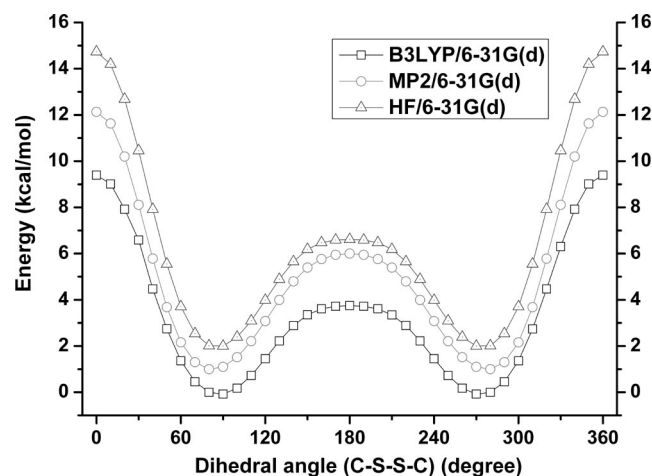


Figure 2. Conformational-energy profile for FC(O)SSCN obtained by using the relaxed scan of the potential energy surface (rotating the CSSC dihedral angle in steps of  $10^\circ$ ) at the HF/6-31G(d), MP2/6-31G(d), and B3LYP/6-31G(d) levels. The curves of MP2/6-31G(d) and HF/6-31G(d) levels are shifted by 1 and 2 kcal/mol, respectively.

When considering the relative orientation of the FC(O) moiety with respect to the S–S bond, which can also be synperiplanar (sp) or antiperiplanar (ap), two possible conformers exist for the title molecule. After structural optimization and vibrational analysis, two conformers of FC(O)SSCN are found to be stable (Figure 1). The relative Gibbs free energies ( $\Delta G$ ) calculated at 298 K for the two stable conformers of FC(O)SSCN after optimization are summarized in Table 1. According to these relative Gibbs free energies the *gauche* (sp) conformer is expected to be the most stable. The stabilization of the *gauche* (sp) conformer can be explained in two ways.<sup>[19]</sup> The first reason is the effect of S–S lone-pair repulsion. The other is the anomeric effect, which is commonly used to describe the preference for the *gauche* conformation exhibited by R–X–A–Y moieties; when A (e.g. C) is an element of medium electronegativity, Y (e.g. O) is more electronegative than A, and X (e.g. S) is an element with lone pairs.<sup>[20]</sup> These effects contribute to the preference for the *gauche* (sp) form of the conformation of the title molecule.

To gain some insight into the stability of these two conformers, NBO calculations<sup>[21–25]</sup> were performed on the title molecule in its optimized *gauche* (sp) and *gauche* (ap) conformations at the B3LYP/6-311+G(3df) level. The total contribution of the stabilization energy  $E(2)$  is 405.89

Table 1. Calculated relative Gibbs free energies ( $\Delta G$  [kcal/mol];  $T = 298$  K) for different conformers of FC(O)SSCN.

Conformer	HF/6-311+G(d)	B3PW91/6-311++G(3df)	B3LYP/6-311++G(3df)
<i>gauche</i> (sp) <sup>[a]</sup>	0	0	0
<i>gauche</i> (ap)	1.5	1.0	0.9

[a] *gauche* refers to the configuration around the S–S bond. The orientation (sp or ap) refers to the C=O bond with respect to the S–S bond.

kcal/mol for the *gauche* (sp) conformer and 398.07 kcal/mol for the *gauche* (ap) conformer, which indicate that the *gauche* (sp) conformer is favored by charge-transfer interactions. The most important orbital interactions relevant to the conformational properties occur between the S(1) lone pairs,  $lp_{\pi}S$  and  $lp_{\sigma}S$  [the  $lp_{\pi}S$  orbital is parallel to the  $\pi(C1-O)$  bond, whereas the  $lp_{\sigma}S$  orbital is not parallel to the  $\pi(C1-O)$  bond], in the vicinity of the C=O [*gauche* (sp) conformer] and C–F [*gauche* (ap) conformer] bonds, and the FC(O) moiety. The stabilization energies for orbital interactions are listed in Table 2. The strongest interaction describing a mesomeric effect (conjugation) is that between the  $lp_{\pi}S(1)$  lone pair and the  $\pi^*(C1-O)$  bond [ $lp_{\pi}S(1) \rightarrow \pi^*(C1-O)$ ], which results in the FC(O)S moiety being a planar structure in both conformers. The  $lp_{\sigma}S(1)$  lone pair can interact either with the  $\sigma^*(C1-O)$  orbital in the sp form or with the  $\sigma^*(C1-F)$  orbital in the ap form (anomeric effect). The sum of these orbital-interaction energies favors the sp form by 2.81 for FC(O)SCI and 2.86 for FC(O)SSCN. For FC(O)SCI the most stable conformer is the sp species, which is also confirmed by gas electron diffraction (GED) studies.<sup>[2,19]</sup> The analysis above indicates that the sp conformer of FC(O)SSCN is more stable. Our discussion of the geometric and electronic structures of the title molecule will mainly focus on the theoretically most stable conformers.

Table 2. Stabilization energies<sup>[a]</sup> for orbital interactions between  $lp_{\pi}S(1)$  and  $lp_{\sigma}S(1)$  sulfur lone pairs with  $\pi^*(C1-O)$ ,  $\sigma^*(C1-O)$ , and  $\sigma^*(C1-F)$  for synperiplanar (sp) and antiperiplanar (ap) conformers and relative total energies for the FC(O)SSCN and FC(O)SCI.

	FC(O)SCI <sup>[19]</sup>		FC(O)SSCN <sup>[b]</sup>	
	sp	ap	sp	ap
$lp_{\sigma}S(1) \rightarrow \sigma^*(C1-O)$ (for sp)	5.8	3.3	4.91	2.88
$lp_{\sigma}S(1) \rightarrow \sigma^*(C1-F)$ (for ap)				
$lp_{\pi}S(1) \rightarrow \pi^*(C1-O)$	28.32	28.01	28.52	27.69
$\Delta E_{\text{anom}}^{\text{int}}$ [c]	2.5		2.03	
$\Delta E_{\text{conj}}^{\text{int}}$ [d]	0.31		0.83	
$\Delta E_{\text{total}}^{\text{int}}$ [e]	2.81		2.86	

[a] [kcal/mol]. [b] Using B3LYP/6-311+G(3df) approximation. [c]  $\Delta E_{\text{anom}}^{\text{int}}$  = anomeric interaction energy difference of the sp and ap conformers. [d]  $\Delta E_{\text{conj}}^{\text{int}}$  = conjugation interaction energy difference of the sp and ap conformers. [e]  $\Delta E_{\text{total}}^{\text{int}} = \Delta E_{\text{anom}}^{\text{int}} + \Delta E_{\text{conj}}^{\text{int}}$ .

The optimized geometries of the *gauche* (sp) conformer of FC(O)SSCN are listed at different levels in Table 3.

In several molecules containing triatomic pseudohalide groups, e.g. SCN, NCO, NNN, etc., it has been established that the atoms are not colinear.<sup>[26,27]</sup> In combination with the FC(O)S moiety, the SCN angle shows about 4° deviation from linearity, which is similar to those found for XSCN species (X = CN,<sup>[28]</sup> SCN,<sup>[29]</sup> Cl<sup>[30]</sup>). The calculated

Table 3. Optimized geometric parameters for the *gauche* (sp) conformer of FC(O)SSCN and FC(O)SSCN<sup>+</sup>.<sup>[a]</sup>

	FC(O)SSCN B3LYP <sup>[b]</sup>	FC(O)SSCN <sup>+</sup> UB3LYP <sup>[b]</sup>
$r_{FC1}$	1.347	1.298
$r_{OC1}$	1.174	1.166
$r_{C1S1}$	1.780	1.875
$r_{S1S2}$	2.071	2.037
$r_{S2C2}$	1.695	1.675
$r_{C2N}$	1.155	1.160
$a_{FC1O}$	123.5	129.6
$a_{FC1S1}$	105.9	106.1
$a_{C1S1S2}$	101.4	93.8
$a_{S1S2C2}$	102.1	99.4
$a_{S2C2N}$	175.7	174.5
$\delta_{OC1S1S2}$	−2.6	0
$\delta_{C1S1S2C2}$	89.5	180
$\delta_{S1S2C2N}$	175.1	180

[a] Distances [Å], angles [°]. For atom numbering see Figure 1. [b] Basis set: 6-311+G(3df).

S–C and C–N bond lengths are also close to the previously reported values.<sup>[18]</sup>

S–S bond lengths,  $r_{SS}$ , and dihedral angles,  $\delta_{CSSC}$ , of known disulfides XSSY are summarized in Table 4. According to a theoretical calculation, the S–S bond length of FC(O)SSCN is 2.071 Å [B3LYP/6-311+G(3df)], which is similar to that of other disulfides substituted with carbon-containing groups. This observation was rationalized with the anomeric effect.<sup>[19]</sup> The anomeric interaction  $lp(S) \rightarrow \sigma^*(S-C)$  for carbon-substituted groups bonded to the disulfide bond is similar in these compounds, leading to similar disulfide bond lengths.

Besides the S–S bond length, another important structural parameter for dichalcogenides is the torsional angle,  $\delta_{XSSY}$ , which greatly influences the whole structure of the molecules. Gas-phase structures of noncyclic disulfides XSSY are characterized by dihedral angles,  $\delta_{XSSY}$ , close to 90° (Table 4). A plausible interpretation of the population analysis is related to the resulting barrier formed by the repulsion of the  $3p\pi$ -AO lone pairs.<sup>[42,43]</sup> The repulsion is minimized if these AOs are oriented orthogonal to each other. The second argument<sup>[42,43]</sup> is based on a hyperconjugative mechanism, whereby the  $\pi$ -character of the S–S bond is enhanced; for example in HSSH the S–H bonds are aligned for maximum transfer of electron density through the  $3p\pi$ -AOs to the hydrogen atom, like in  $H-S^+=SH^-$ . This feature is consistent with the anomeric effect, that is, the electron donation from the sulfur lone pair into the empty  $\sigma^*$ -orbitals of the opposite S–H bonds.<sup>[21]</sup> For other alkyl<sup>[44]</sup> and nonalkyl-substituted<sup>[39,45]</sup> species a similar feature was observed.

Table 4. S–S bond lengths and dihedral angles  $\delta_{\text{XSSY}}$  in known disulfides.<sup>[a]</sup>

XSSY	$r_{\text{SS}}$	$\delta_{\text{XSSY}}$	Method
HSSH <sup>[16]</sup>	2.0564	90.34	millimeter wave
FSSF <sup>[31]</sup>	1.890(2)	87.7(4)	GED
CISSCI <sup>[32]</sup>	1.931(5)	84.8(13)	GED
CISSCN <sup>[18]</sup>	2.018	84.60	MP2/6-311G(3df)
CCl <sub>3</sub> SSCN <sup>[33]</sup>	2.061	91.4	B3LYP/6-311+G(3df)
CH <sub>3</sub> SSCH <sub>3</sub> <sup>[34]</sup>	2.029(3)	85.3(37)	GED
CF <sub>3</sub> SSCF <sub>3</sub> <sup>[35]</sup>	2.030(5)	104.4(40)	GED
CF <sub>3</sub> SSNSO <sup>[36]</sup>	2.016(4)	81.3(94)	GED
FC(O)SSCH <sub>3</sub> <sup>[6]</sup>	2.035	83.5(1.5)	microwave spectrum
FC(O)SSCN <sup>[b]</sup>	2.071	89.5	B3LYP/6-311+G(3df)
FC(O)SSCF <sub>3</sub> <sup>[37]</sup>	2.027(4)	95.0(27)	GED
CH <sub>3</sub> OC(O)SSCN <sup>[10]</sup>	2.075	80.5	MP2/6-311++G(d,p)
CH <sub>3</sub> OSSOCH <sub>3</sub> <sup>[38]</sup>	1.9719(8)	81.48(5)	X-ray
FC(O)SSC(O)F <sup>[39]</sup>	2.028(4)	82.2(19)	GED
FC(O)SSC(O)CF <sub>3</sub> <sup>[7]</sup>	2.023(3)	77.7(21)	GED
FC(O)SSC(O)CF <sub>2</sub> Cl <sup>[40]</sup>	2.029(1)	84.2(2)	X-ray
CH <sub>3</sub> C(O)OSSOC(O)CH <sub>3</sub> <sup>[17]</sup>	1.959	−93.1	B3LYP/6-311++G(3df,3pd)
CF <sub>3</sub> C(O)OSSOC(O)CF <sub>3</sub> <sup>[41]</sup>	1.979	−95.1	B3LYP/6-311G(d)

[a] Distances [Å], angles [°]. [b] This work.

### Photoelectron Spectroscopy

Photoelectron spectroscopy with a He I resonance source (58.4 nm) is an efficient method for investigating the valence electronic structure of unstable species in combination with DFT calculations.<sup>[10,18,17,46]</sup> The He I photoelectron spectrum of FC(O)SSCN is presented in Figure 3. Before assigning the spectrum, outer-valence Green's function (OVGF)<sup>[47]</sup> calculations were carried out to obtain the ionization energies for FC(O)SSCN. The experimental vertical ionization energies (*IE* in eV), theoretical vertical ionization energies ( $E_v$  in eV), molecular orbitals, and corresponding characters of outer-valence shells for FC(O)SSCN are listed in Table 5. Table 5 shows that the OVGF pole strengths are all larger than 0.85, which is consistent with a one-electron depiction of ionization. Note that if the OVGF pole strengths are smaller than 0.85 then a severe breakdown of the orbital (or one-electron) picture of ionization should be expected, and the OVGF approach would no longer be applicable.<sup>[48–50]</sup> Drawings of nine MOs for FC(O)SSCN are shown in Figure 4.

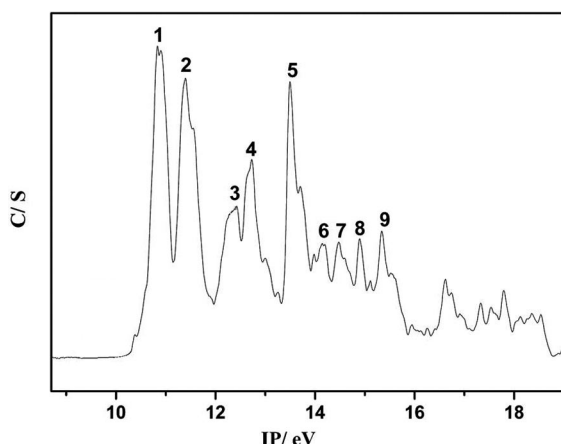


Figure 3. He I photoelectron spectrum (PES) of FC(O)SSCN.

Table 5. Experimental and calculated ionization energies and MO characters for FC(O)SSCN.<sup>[a]</sup>

Band	Exp. <i>IE</i>	Calcd. $E_v$ <sup>[b,c]</sup>	MO	Character
1	10.89	10.97 (0.90)	34	$n_{\text{S}(\text{SCN})}, \pi_{\text{C}=\text{N}}$
2	11.39	11.37 (0.89)	33	$n_{\text{S}[\text{FC}(\text{O})\text{S}]}$
3	12.42	12.73 (0.88)	32	$\pi_{\text{C}=\text{N}}$
4	12.73	12.79 (0.89)	31	$n_{\text{O}}$
5	13.50	14.13 (0.87)	30	$\sigma_{\text{C}=\text{N}}$
6	14.17	14.24 (0.87)	29	$\pi_{\text{C}=\text{O}}, n_{\text{F}}$
7	14.48	14.59 (0.88)	28	$\pi_{\text{SCN}}$
8	14.89	14.95 (0.87)	27	$\sigma_{\text{SS}}, \pi_{\text{SCN}}$
9	15.36	15.68 (0.88)	26	$n_{\text{F}}$

[a] Energies [eV]. [b] OVGF from geometries at the B3LYP/6-311+G(3df) level. [c] Pole strength in parentheses.

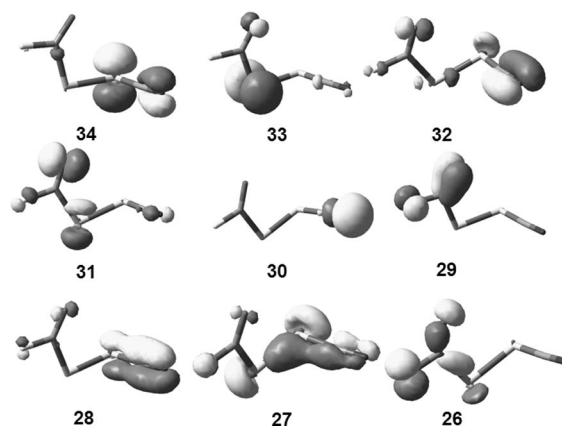


Figure 4. Characters of the occupied molecular orbitals for FC(O)SSCN.

In the photoelectron spectrum of FC(O)SSCN the ionization energies of different bands are in good agreement with the calculated values of the OVGF method. The first two peaks in the photoelectron spectrum of FC(O)SSCN are centered at 10.89 and 11.39 eV. The main characters for the first two outermost orbitals are  $\{34[n_{\text{S}(\text{SCN})}, \pi_{\text{C}=\text{N}}]\}^{-1}$



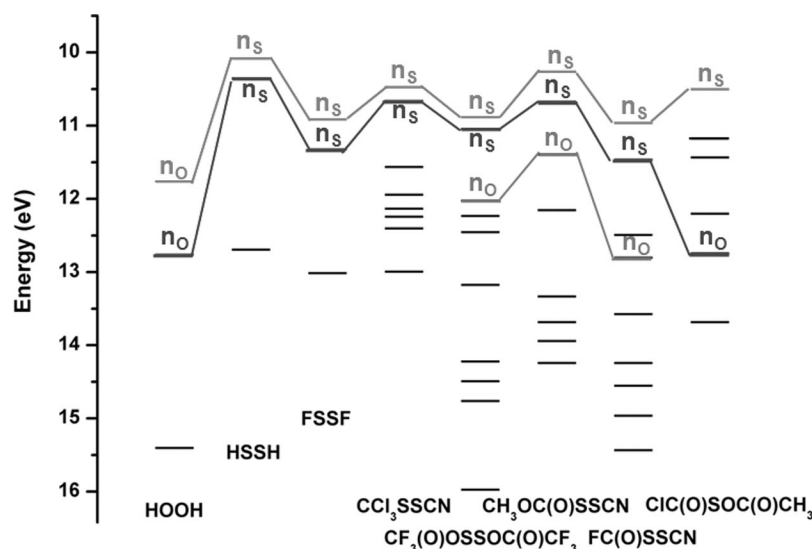


Figure 5. Correlation between selected dichalcogenides. The ionization energies of HOOH, HSSH, FSSF,  $\text{CCl}_3\text{SSCN}$ ,  $\text{CF}_3\text{C}(\text{O})\text{OSSOC}(\text{O})\text{CF}_3$ ,  $\text{CH}_3\text{OC}(\text{O})\text{SSCN}$ ,  $\text{FC}(\text{O})\text{SSCN}$ , and  $\text{ClC}(\text{O})\text{SOC}(\text{O})\text{CH}_3$  are taken from refs.<sup>[55,54,33,41,10,56]</sup>, respectively.

and  $(33\{n_{\text{S}[\text{FC}(\text{O})\text{S}]}\})^{-1}$ . The energy difference  $\Delta E$  between the first two bands in  $\text{FC}(\text{O})\text{SSCN}$  is 0.50 eV, which is similar to that of  $\text{FC}(\text{O})\text{SSCH}_3$  [ $\Delta E = 0.3$  eV,  $\delta_{\text{CSSC}} = 83.5(1.5)^\circ$ ].<sup>[2]</sup> As pointed out by Baker et al.,<sup>[51,52]</sup> for disulfides, peroxides, and diselenides, the first two bands in the photoelectron spectra correspond to the symmetric and antisymmetric linear combinations of the  $\text{S}_{3p}$  atomic orbitals. In general, it is expected that as the dihedral angle  $\delta_{\text{CSSC}}$  deviates from  $90^\circ$  the energy separation  $\Delta E$  between the  $\pi$ - and  $\pi^*$ -orbitals will increase, i.e. the  $3p$ -orbitals in a parallel configuration ( $\delta = 0, 180^\circ$ ) interact more strongly than they do in an orthogonal configuration ( $\delta = 90^\circ$ ).<sup>[43]</sup> The difference between the two bands finds its origin in the interaction of the two sulfur lone pairs, and is very much dependent on the CSSC dihedral angle. In general, the pattern of the splitting is predicted to be  $\Delta(\text{OO}) > \Delta(\text{SS}) \approx \Delta(\text{SeSe})$  for homonuclear systems and  $\Delta(\text{SO}) > \Delta(\text{SeS})$  for heteronuclear ones. Also, the differences in heteronuclear systems are much larger than those observed in homonuclear systems.<sup>[53]</sup> The successive replacement of O by S and Se induces only a progressively minor perturbation of the electronic structure, as is expected from the electronegativity sequence of the chalcogens; O (3.5 on Pauling's scale), S (2.5), and Se (2.4).<sup>[48]</sup> The correlation between selected dichalcogenides is shown in Figure 5. The ionization process from the lone pairs of two S atoms is 0.5 eV, which is close to those of the parent compounds, HSSH (0.27 eV),<sup>[54]</sup> FSSF (0.41 eV),<sup>[54]</sup> and  $\text{CH}_3\text{OC}(\text{O})\text{SSCN}$  (0.41 eV)<sup>[10]</sup> (Figure 5). These energy differences are smaller than those of heteronuclear systems.

In the case of  $\text{FC}(\text{O})\text{SSCN}$  the electronegativity of the  $\text{FC}(\text{O})$  moiety is stronger than that of the  $\text{C}\equiv\text{N}$  group. Thus, the first band at 10.89 eV can merely be attributed to the S lone pair at the sulfur atom bonded to the  $\text{C}\equiv\text{N}$  group, and the second band, at 11.39 eV, to the S lone pair of the sulfur atom bonded to the  $\text{FC}(\text{O})$  moiety. The result

is similar to that of  $\text{FC}(\text{O})\text{SSCH}_3$ <sup>[2]</sup> and  $\text{CH}_3\text{OC}(\text{O})\text{SSCN}$ .<sup>[10]</sup>

Another important functional group in  $\text{FC}(\text{O})\text{SSCN}$  is the SCN moiety, which can greatly influence the electronic structure of the whole molecule. The first, third, fifth, seventh, and eighth bands correspond to different orbitals on the SCN moiety. In most cases the spectra of pseudohalides are somewhat more complicated. The electronic structure of the SCN moiety can be explained in two ways.<sup>[18]</sup> One can assume a single S–C bond and a triple  $\text{C}\equiv\text{N}$  bond. In this case, the appearance of two new bands resulting from the  $\text{C}\equiv\text{N}$   $\pi$ -band is expected in the low-energy region of the spectrum. The corresponding bands in the photoelectron spectrum are located at 10.89 and 12.42 eV and can be attributed to the  $\{34[n_{\text{S}(\text{SCN})}, \pi_{\text{C}\equiv\text{N}}]\}^{-1}$  and  $[32(\pi_{\text{C}\equiv\text{N}})]^{-1}$  one-electron ionization lines, respectively. Another interpretation is that the SCN unit is considered to be a two-perpendicular four-electron, three-center  $\pi$ -system, which suggests four new bands in the spectrum (the high-energy  $\pi_{\text{SCN}}$  and  $\pi_{\text{SCN}\perp}$  and the low-energy  $\pi_{\text{C}\equiv\text{N}}$  and  $\pi_{\text{C}\equiv\text{N}\perp}$ ). If the molecular skeleton was linear, the perpendicular MO pairs should be degenerate. When the S–S bond is bent, four non-degenerate  $\pi$ -bonds are expected. Therefore, the corresponding bands in the photoelectron spectrum are located at 10.89, 12.42, 14.48, and 14.89 eV and relate to the  $\{34[n_{\text{S}(\text{SCN})}, \pi_{\text{C}\equiv\text{N}}]\}^{-1}$ ,  $[32(\pi_{\text{C}\equiv\text{N}})]^{-1}$ ,  $[28(\pi_{\text{SCN}})]^{-1}$ , and  $[27(\sigma_{\text{SS}}, \pi_{\text{SCN}})]^{-1}$  one-electron ionization lines, respectively.

The fourth band in the photoelectron spectrum of  $\text{FC}(\text{O})\text{SSCN}$  can be attributed to the oxygen lone pair ( $n_{\text{O}}$ ) electron of the  $\text{C}=\text{O}$  group, with a large contribution from the  $3p$  in-plane orbital of the sulfur atom (Figure 4). In the case of acetyl fluoride, formyl fluoride,  $\text{FC}(\text{O})\text{SCl}$ ,  $\text{CF}_3\text{C}(\text{O})\text{OSSOC}(\text{O})\text{CF}_3$ , and  $\text{CH}_3\text{OC}(\text{O})\text{SSCN}$ , the corresponding bands are found at 11.3, 12.6, 12.1, 11.95, and 11.32 eV, respectively. For cyanofluoride  $[\text{FC}(\text{O})\text{CN}]$  this orbital appears at 13.2 eV because of the strong induc-

tive effect of the cyano group.<sup>[55]</sup> The analysis above demonstrates that the fourth band depends on the atoms bonded to both the carbon and the sulfur atoms (Figure 4).

The ionization from the orbital mainly localized at the  $\sigma$ -bond of the SS group causes the ionization energy of 14.89 eV in FC(O)SSCN. It is higher than the corresponding ionization energies of HSSH (12.62 eV),<sup>[54]</sup> FSSF (12.94 eV),<sup>[54]</sup> CCl<sub>3</sub>SSCN (12.06 eV),<sup>[33]</sup> and CH<sub>3</sub>OC(O)-SSCN (12.08 eV).<sup>[10]</sup> The differences are caused by the effect of the different substituents on the S–S bond. Figure 4 shows that strong interactions occur between the  $\sigma_{SS}$ - and  $\pi_{SCN}$ -orbitals.

The sixth and ninth bands in the photoelectron spectrum arise from ionizations related to the FC(O) moiety. The planar geometry of the group allows interactions between the  $\pi_{C=O}$  and  $n_F$  localized orbitals to become effective. Such an interaction is not possible for the in-plane  $n_F$  lone-pair orbital (Figure 4). Thus, the band at 14.17 eV may involve  $\pi_{C=O}$ - and  $n_F$ -orbitals. The structureless band at 15.36 eV can be related to the in-plane  $n_F$ -orbital. The corresponding bands of formyl fluoride<sup>[57,58]</sup> and propynoyl fluoride<sup>[59]</sup> are found at 15.5 and 15.4 eV, respectively, which exhibit remarkably similar shapes.

The bands in the higher ionization region, above 16.0 eV, show a broad feature making it difficult for further assignments.

### Photoionization Mass Spectrum

The reaction process for generating FC(O)SSCN was monitored by photoionization mass spectrometry. The ultraviolet photoionization mass spectrum of the reaction products of gaseous FC(O)SCl and AgSCN at room temperature is shown in Figure 6. The analysis of the PIMS results becomes easier when combined with both the PES and theoretical results. The spectrum of FC(O)SSCN (Fig-

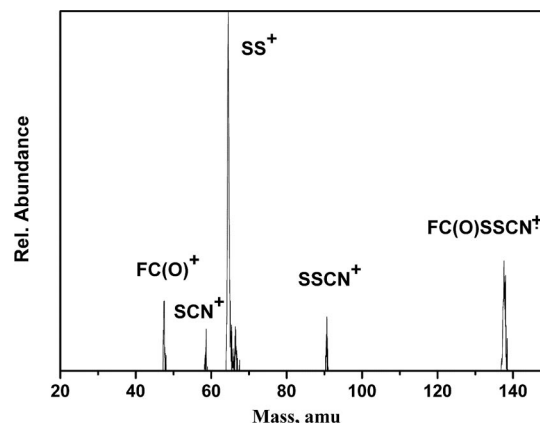


Figure 6. He I photoionization mass spectrum of FC(O)SSCN.

Table 6. Calculated and experimental ionization energies of FC(O)SSCN and its fragments.

Molecule	Energy <sup>[a]</sup> [hartree]	<i>IE</i> <sup>[a]</sup> [eV] (calcd.)	<i>IE</i> [eV] (exp.)
FC(O)SSCN	–1102.56569529	10.02	10.07 <sup>[b]</sup>
FC(O)SSCN <sup>+</sup>	–1102.19761350		
FC(O) <sup>+</sup>	–213.18362312	9.48	≤ 9.7 <sup>[60]</sup>
FC(O) <sup>+</sup>	–212.8353579		
FC(O)SS <sup>+</sup>	–1009.68514530	9.79 <sup>[b]</sup>	/
FC(O)SS <sup>+</sup>	–1009.32545494		
FC(O)S <sup>+</sup>	–611.43941069	10.93 <sup>[b]</sup>	/
FC(O)S <sup>+</sup>	–611.03773198		
CN <sup>+</sup>	–92.74465710	14.05	14.2 ± 0.3 <sup>[61]</sup>
CN <sup>+</sup>	–92.22848457		
SSCN <sup>+</sup>	–889.28719827	9.96 <sup>[b]</sup>	/
SSCN <sup>+</sup>	–888.92131425		
SS <sup>+</sup>	–796.43324028	9.54	9.5 ± 0.2 <sup>[62]</sup>
SS <sup>+</sup>	–796.08256073		
S <sup>+</sup>	–398.1344981	10.54	10.4 ± 0.3 <sup>[63]</sup>
S <sup>+</sup>	–397.7469576		
SCN <sup>+</sup>	–491.05221809	10.61	10.689 ± 0.005 <sup>[64]</sup>
SCN <sup>+</sup>	–490.66212748		

[a] B3LYP/6-311+G(3df). [b] This work.

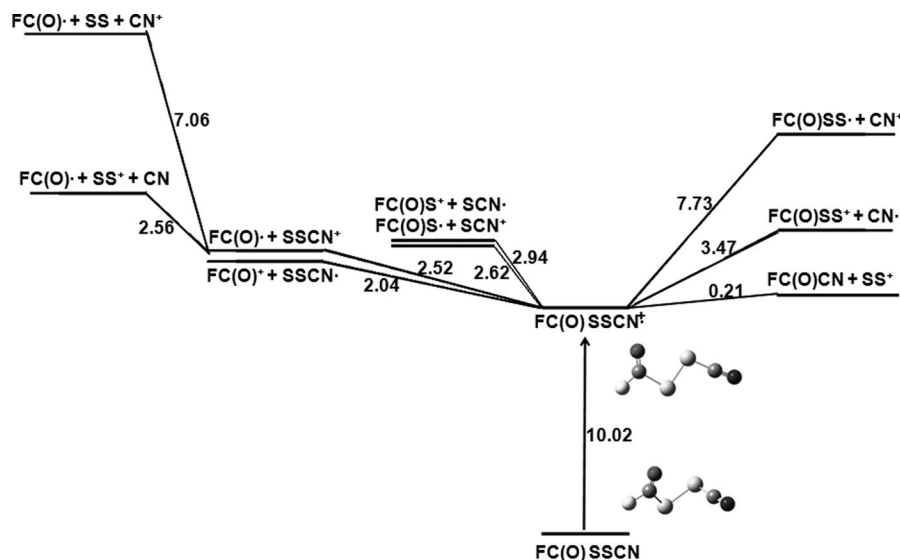


Figure 7. Schematic energy profile [eV] showing ionization and dissociation pathways of FC(O)SSCN calculated at the B3LYP/6-311+G(3df) level.

ure 6) shows five peaks:  $\text{FC(O)}^+$ ,  $\text{SCN}^+$ ,  $\text{SS}^+$ ,  $\text{SSCN}^+$ , and the parent ion. In order to validate the level of electronic structure theory used in the energetics calculation of dissociation pathways we computed the adiabatic ionization of  $\text{FC(O)SSCN}$  from the energies of the identified fragments. The calculated results are shown in Table 6 along with the experimentally measured values. There are no data available on the experimental  $IE$ s of the  $\text{FC(O)SS}^\cdot$ ,  $\text{FC(O)S}^\cdot$ , and  $\text{SSCN}^\cdot$  radicals. Since the calculated and experimental  $IE$ s of the other fragments are in very good agreement, our calculated  $IE$ s for these radicals should be very good estimates of the actual values. These  $IE$ s are necessary to construct the energy diagrams of the dissociation pathway shown in Figure 7. With the assumption of the absence of any significant energy barriers it leads to a fragmentation distribution governed by the energetics of the various product states.

### Ionization and Dissociation

Upon ionization, the CSSC dihedral angle in  $\text{CH}_3\text{SSCH}_3$  [85.1(4°)] is expected to change to 180° in the ground state, and this most stable conformer exhibits  $C_{2h}$  *trans* symmetry. Interestingly, a stable structure with a  $C_{2v}$  symmetry (*cis*- $\text{CH}_3\text{SSCH}_3^{+\cdot}$ ,  $\delta_{\text{CSSC}} = 0^\circ$ ) is also found, and it lies only 0.17 eV above the ground  $C_{2h}$  structure.<sup>[65]</sup> Recently, the structures of ground-state  $\text{FC(O)SSCH}_3^{+\cdot}$  have been studied by Erben et al.<sup>[66]</sup> It was concluded that after ionization the  $\delta_{\text{CSSC}}$  dihedral angle adopts a value of 180°. Enlightened by both studies, we located the most stable conformers of the ground cation-radical form of  $\text{FC(O)SSCN}^{+\cdot}$  (Figure 1) at the UB3LYP/6-311+G(3df) level of theory. The most stable conformer of  $\text{FC(O)SSCN}^{+\cdot}$  adopts a *trans* conformer with respect to the  $\delta_{\text{CSSC}}$  dihedral angle and has a planar main-atom structure (180°) with  $C_s$  symmetry. This result is similar to that of the molecules we mentioned above. It can be explained that the unpaired electrons of the sulfur atoms are in an antibonding  $\pi^*$ -orbital perpendicular to the plane CSSC in the ground cation-radical form, and that the  $p_z^1$  and  $p_z^2$  components of the  $\pi^*$ -orbital forms the two-center three-electron  $\pi$ -bond. This  $\pi$ -bond is parallel to the S–S bond.<sup>[67–69]</sup>

The geometry [UB3LYP/6-311+G(3df)] of the planar  $C_s$ -symmetry conformer of the radical-cation  $\text{FC(O)SSCN}^{+\cdot}$  in its ground state is compared with that of the neutral molecule in Table 3.

An interesting and important feature of  $\text{FC(O)SSCN}^{+\cdot}$  is the changes in bond lengths with regard to the  $r_{\text{CIS1}}$  and  $r_{\text{SIS2}}$  bonds: the  $r_{\text{CIS1}}$  bond elongates to 1.875 Å and the  $r_{\text{SIS2}}$  bond shortens by 0.034 Å after ionization. These changes in the geometric parameters are most strongly influenced by the removal of the  $\sigma_{\text{CIS1}}$  and  $\sigma_{\text{S2C2}}$  bonding electrons. Because of the formation of the two-center three-electron  $\pi$  bond the S–S bond possesses some double-bond properties and shortens. These results suggest that the parent ion is more strongly subject to a dissociation of the C1–S1 single bond to form the  $\text{FC(O)}^\cdot + \text{SSCN}^+$  pair or the  $\text{FC(O)}^+ + \text{SSCN}^\cdot$  pair. The possible dissociation pathways

for  $\text{FC(O)SSCN}$  are presented in Figure 7. As can be seen, the energy for the dissociation of the parent ion to the  $\text{FC(O)}^+ + \text{SSCN}^\cdot$  pair (2.04 eV) is lower than that for the dissociation into the  $\text{FC(O)}^\cdot + \text{SSCN}^+$  pair (2.52 eV). It is worth mentioning that the intermedial  $\text{SSCN}^+$  cation is not very stable and dissociates to generate the  $\text{SS}^+ + \text{CN}^\cdot$  pair. Therefore, as shown in Figure 3, the intensities of  $\text{SS}^+$  and  $\text{FC(O)}^+$  are higher than that of  $\text{SSCN}^+$ , and the  $\text{FC(O)CN} + \text{SS}^+$  pair (0.21 eV) might form through an intermolecular conversion. These results might indicate the reason for  $\text{SS}^+$  having the strongest intensity. Moreover, as shown in Figure 7, the energy of the direct dissociation of the S–S bond in the parent ion to generate  $\text{SCN}^+$  (2.62 eV) is lower than that required for the formation of the  $\text{FC(O)S}^+ + \text{SCN}^\cdot$  pair (2.94 eV), and the energy of the  $\text{FC(O)S}^\cdot + \text{SCN}^+$  pair (2.62 eV) generation is similar to that of the  $\text{FC(O)}^\cdot + \text{SSCN}^+$  pair (2.52 eV). These results may explain why the intensities of the  $\text{SCN}^+$  and  $\text{SSCN}^+$  species are similar without the peak of  $\text{FC(O)S}^+$ .

### Conclusions

Fluorocarbonylsulfur thiocyanate [ $\text{FC(O)SSCN}$ ] was generated and characterized by photoelectron spectroscopy (PES) and photoionization mass spectrometry (PIMS). With the help of quantum chemical calculations, the geometry of the title molecule was investigated, and the electronic structure was analyzed. The title compound prefers a *gauche* conformation as predicted by structural optimization and vibrational analysis. After ionization, the cationic-radical form [ $\text{FC(O)SSCN}^{+\cdot}$ ] adopts a *trans*-planar main-atom structure with  $C_s$  symmetry. The  $r_{\text{CIS1}}$  bond elongates to 1.875 Å and the  $r_{\text{SIS2}}$  bond is shortened by 0.034 Å after ionization. This ionization corresponds to the leaving electrons mainly localized on the sulfur 3p lone-pair orbitals:  $\{34[n_{\text{S}(\text{SCN})}, \pi_{\text{C}\equiv\text{N}}]\}^{-1}$  and  $\{33[n_{\text{S}(\text{FC(O)S})}]\}^{-1}$ , with an energy separation of 0.50 eV. The first vertical ionization energy is 10.89 eV, which is unidentical with the first adiabatic ionization energy of 10.07 eV because of the geometric change after ionization. With these analyses and theory calculations we presented an investigation of the possible ionization and dissociation processes.

### Experimental Section

**Sample Preparation:** Silver thiocyanate was found to be an ideal precursor for the preparation of thiocyanates.<sup>[29,70,18]</sup> In this work, fluorocarbonylsulfur thiocyanate [ $\text{FC(O)SSCN}$ ] was heterogeneously generated at room temperature by passing fluorocarbonylsulfur chloride [ $\text{FC(O)SCI}$ ] vapor over finely powdered silver thiocyanate ( $\text{AgSCN}$ ), and in situ photoelectron and photoionization mass spectra were recorded after its generation. The reaction route is illustrated in Equation (1).



The precursor  $\text{FC(O)SCI}$  was prepared according to a previous report,<sup>[71]</sup> and its PE and IR spectra are identical to those recorded



previously.<sup>[13,72]</sup> AgSCN was purchased from Alfa Aesar Company, and its purity was > 99%. Before reaction, silver thiocyanate was dried in vacuum ( $1 \times 10^{-4}$  Torr) for 2 h.

**Instrumentation:** The experimental apparatus used in this work has been described previously.<sup>[10,41,73]</sup> Briefly, the photoelectron and photoionization mass spectrometer consists of two parts: one part is the double-chamber UPS-II machine;<sup>[74]</sup> the other is a time-of-flight mass spectrometer. The PES was recorded with the double-chamber UPS-II machine, which was built specifically to detect transient species at a resolution of about 30 meV as indicated by the Ar<sup>+</sup> (<sup>2</sup>P<sub>3/2</sub>) photoelectron band. Experimental vertical ionization energies were calibrated by the simultaneous addition of a small amount of argon and methyl iodide to the sample. Mass analysis of ions was achieved with the time-of-flight mass analyzer mounted directly to the photoionization point. The relatively soft ionization is provided by single-wavelength He I radiation. The PE and PIM spectra can be recorded within seconds of each other under identical conditions.

**Quantum Chemical Calculations:** Electronic structure calculations were carried out by using the Gaussian 03 program package.<sup>[75]</sup> The structure parameters of the neutral molecule and the cation-radical form of FC(O)SSCN were optimized with ab initio and DFT methods. Higher levels of theory were used to optimize the theoretically most stable conformers. Relaxed scans of the potential energy surface were performed to search for other possible conformers of FC(O)SSCN at the HF/6-31G(d), MP2/6-31G(d), and B3LYP/6-31G(d) levels. The natural bond orbital (NBO) calculations were performed at the B3LYP/6-311+G(3df) level by using the NBO 3.1 code as implemented in the Gaussian 03 program package. To assign the PES of FC(O)SSCN, we applied the OGVF approach with a 6-311+G(3df) basis set, which includes sophisticated correlation effects of the self-energy to the molecules to give accurate results of the vertical ionization energies.<sup>[47]</sup> Three-dimensional MO plots were obtained with the Gauss View program by using the 0.08 isodensity.

## Acknowledgments

This project was supported by the 973 program of the Ministry of Science and Technology of China (No. 2006CB403701), Knowledge Innovation Program of the Chinese Academy of Sciences (Grant No. KZCX2-YW-205), and the National Natural Science Foundation of China (Contract No. 20577052, 20673123).

- [1] H.-G. Mack, H. Oberhammer, C. O. Della Védova, *J. Phys. Chem.* **1991**, 95, 4238–4241.
- [2] M. F. Erben, C. O. Della Védova, *Inorg. Chem.* **2002**, 41, 3740–3748.
- [3] I. V. Koval', *Russ. Chem. Rev.* **1994**, 63, 735–750.
- [4] A. Rietsch, J. Beckwith, *Annu. Rev. Genet.* **1998**, 32, 163–184.
- [5] A. Hermann, S. E. Ulic, C. O. Della Védova, H.-G. Mack, H. Oberhammer, *J. Fluorine Chem.* **2001**, 112, 297–305.
- [6] A. C. Fantoni, C. O. Della Védova, *J. Mol. Spectrosc.* **1992**, 154, 240–245.
- [7] M. F. Erben, C. O. Della Védova, H. Willner, F. Trautner, H. Oberhammer, R. Boese, *Inorg. Chem.* **2005**, 44, 7070–7077.
- [8] E. Söderbäck, *Justus Liebigs Ann. Chem.* **1919**, 419, 217–322.
- [9] Z. Ajji, D. Y. Naima, M. N. Odeh, A. W. Allaf, *Spectrochim. Acta Part A* **1999**, 55, 1753–1756.
- [10] L. Du, L. Yao, M. F. Ge, *Eur. J. Inorg. Chem.* **2007**, 4514–4519.
- [11] C. J. Marsden, F. D. Brown, P. D. Godfrey, *J. Chem. Soc., Chem. Commun.* **1979**, 399–401.
- [12] F. Fehér, H. Weber, *Chem. Ber.* **1958**, 91, 642–650.
- [13] A. Haas, H. Reinke, *Chem. Ber.* **1969**, 102, 2718–2727.
- [14] A. Haas, H. Reinke, *Angew. Chem. Int. Ed. Engl.* **1967**, 6, 705–706.
- [15] C. J. Marsden, B. J. Smith, *J. Phys. Chem.* **1988**, 92, 347–353.
- [16] G. Winnewisser, K. M. T. Yamada, *Vib. Spectrosc.* **1991**, 1, 263–272.
- [17] L. Du, L. Yao, M. F. Ge, *J. Phys. Chem. A* **2007**, 111, 11787–11792.
- [18] L. Yao, M. F. Ge, W. G. Wang, X. Q. Zeng, Z. Sun, D. X. Wang, *Inorg. Chem.* **2006**, 45, 5971–5975.
- [19] M. F. Erben, C. O. Della Védova, R. M. Romano, R. Boese, H. Oberhammer, H. Willner, O. Sala, *Inorg. Chem.* **2002**, 41, 1064–1071.
- [20] A. J. Kirby, *The Anomeric Effect and Related Stereoelectronic Effects at Oxygen*, Springer, Berlin, **1983**.
- [21] T. K. Brunck, F. Weinhold, *J. Am. Chem. Soc.* **1979**, 101, 1700–1709.
- [22] A. E. Reed, L. A. Curtiss, F. Weinhold, *Chem. Rev.* **1988**, 88, 899–926.
- [23] A. E. Reed, F. Weinhold, *J. Chem. Phys.* **1985**, 83, 1736–1740.
- [24] A. E. Reed, R. B. Weinstock, F. Weinhold, *J. Chem. Phys.* **1985**, 83, 735–746.
- [25] E. D. Glendening, A. E. Reed, J. E. Carpenter, F. Weinhold, *NBO*, version 3.1, Gaussian Inc., Pittsburgh, PA, **1992**.
- [26] A. Schulz, I. C. Tornieporth-Oetting, T. M. Klapötke, *Inorg. Chem.* **1995**, 34, 4343–4346.
- [27] T. M. Klapötke, A. Schulz, *Inorg. Chem.* **1997**, 36, 1929–1933.
- [28] P. Rosmus, H. Stafast, H. Bock, *Chem. Phys. Lett.* **1975**, 34, 275–280.
- [29] D. C. Frost, C. Kirby, W. M. Lau, C. B. Macdonald, C. A. McDowell, N. P. C. Westwood, *Chem. Phys. Lett.* **1980**, 69, 1–6.
- [30] D. C. Frost, C. B. MacDonald, C. A. McDowell, N. P. C. Westwood, *J. Am. Chem. Soc.* **1981**, 103, 4423–4427.
- [31] C. J. Marsden, H. Oberhammer, O. Lösing, H. Willner, *J. Mol. Struct.* **1989**, 193, 233–245.
- [32] B. Beagley, G. H. Echersly, D. P. Brown, D. Tomlinson, *Trans. Faraday Soc.* **1969**, 65, 2300–2307.
- [33] L. Du, L. Yao, M. F. Ge, *Chin. J. Chem. Phys.* **2008**, 21, 93–98.
- [34] A. Yokozeki, S. H. Bauer, *J. Phys. Chem.* **1976**, 80, 618–625.
- [35] C. J. Marsden, B. Beagley, *J. Chem. Soc. Faraday Trans. 2* **1981**, 77, 2213–2221.
- [36] R. M. Romano, C. O. Della Védova, A. Pfeiffer, H.-G. Mack, H. Oberhammer, *J. Mol. Struct.* **1998**, 446, 127–135.
- [37] A. Hermann, S. E. Ulic, C. O. Della Védova, H. G. Mack, H. Oberhammer, *J. Fluorine Chem.* **2001**, 112, 297–305.
- [38] T. Koritsanzsky, J. Buschmann, P. Luger, H. Schmidt, R. Steudel, *J. Phys. Chem.* **1994**, 98, 5416–5421.
- [39] H.-G. Mack, C. O. Della Védova, H. Oberhammer, *J. Phys. Chem.* **1992**, 96, 9215–9217.
- [40] M. F. Erben, C. O. Della Védova, H. Willner, R. Boese, *Eur. J. Inorg. Chem.* **2006**, 4418–4425.
- [41] X. Q. Zeng, M. F. Ge, Z. Sun, D. X. Wang, *J. Phys. Chem. A* **2006**, 110, 5685–5691.
- [42] G. Winnewisser, N. Winnewisser, W. Gordy, *J. Chem. Phys.* **1968**, 49, 3465–3478.
- [43] D. B. Boyd, *J. Am. Chem. Soc.* **1972**, 94, 8799–8804.
- [44] H. E. Van Wart, F. Cardinaux, H. A. Scheraga, *J. Phys. Chem.* **1976**, 80, 625–630.
- [45] S. E. Ulic, C. O. Della Védova, P. J. Aymonino, *J. Raman Spectrosc.* **1991**, 22, 675–678.
- [46] X. Q. Zeng, M. F. Ge, L. Du, Z. Sun, D. X. Wang, *J. Mol. Struct.* **2006**, 800, 62–66.
- [47] J. V. Ortiz, *J. Chem. Phys.* **1988**, 89, 6348–6352.
- [48] M. S. Deleuze, *J. Chem. Phys.* **2002**, 116, 7012–7026.
- [49] M. S. Deleuze, *J. Phys. Chem. A* **2004**, 108, 9244–9259.
- [50] M. S. Deleuze, *Chem. Phys.* **2006**, 329, 22–38.
- [51] J. P. Snyder, L. Carlsen, *J. Am. Chem. Soc.* **1977**, 99, 2931–2942.
- [52] A. D. Baker, M. Brisk, M. Gellender, *J. Electron Spectrosc. Relat. Phenom.* **1974**, 3, 227–228.



- [53] V. Galasso, *J. Electron Spectrosc. Relat. Phenom.* **1984**, *34*, 283–289.
- [54] B. Solouki, H. Bock, *Inorg. Chem.* **1977**, *16*, 665–669.
- [55] K. Osafune, K. Kimura, *Chem. Phys. Lett.* **1974**, *25*, 47–50.
- [56] L. Du, L. Yao, M. F. Ge, *J. Mol. Struct.* **2008**, *882*, 146–152.
- [57] W. Von Niessen, S. G. Fougère, D. Janvier, D. Klapstein, *J. Mol. Struct.* **1992**, *265*, 133–142.
- [58] D. Klapstein, *J. Electron Spectrosc. Relat. Phenom.* **1987**, *42*, 149–160.
- [59] D. Klapstein, R. T. O'Brien, *Can. J. Chem.* **1987**, *65*, 683–686.
- [60] T. J. Buckley, R. D. Johnson, R. E. Huie, Z. Zhang, S. C. Kuo, R. B. Klemm, *J. Phys. Chem.* **1995**, *99*, 4879–4885.
- [61] J. Berkowitz, *J. Chem. Phys.* **1962**, *36*, 2533–2539.
- [62] K. H. Lau, R. D. Brittain, D. L. Hildenbrand, *J. Phys. Chem.* **1982**, *86*, 4429–4432.
- [63] S. Smoes, J. Drowart, J. M. Welter, *J. Chem. Thermodyn.* **1977**, *9*, 275–292.
- [64] B. Ruscic, J. Berkowitz, *J. Chem. Phys.* **1994**, *101*, 7975–7988.
- [65] W. K. Li, S. W. Chiu, Z. X. Ma, C. L. Liao, C. Y. Ng, *J. Chem. Phys.* **1993**, *99*, 8440–8444.
- [66] M. F. Erben, C. O. Della Védova, *Helv. Chim. Acta* **2003**, *86*, 2379–2395.
- [67] L. Bonazzola, J.-P. Michaut, J. Roncin, *J. Chem. Phys.* **1985**, *83*, 2727–2732.
- [68] L. Bonazzola, J.-P. Michaut, J. Roncin, *J. Phys. Chem.* **1989**, *93*, 639–642.
- [69] J. J. Butler, T. Baer, S. A. Evans Jr, *J. Am. Chem. Soc.* **1983**, *105*, 3451–3455.
- [70] Y. M. Li, Z. M. Qiao, Q. Sun, J. C. Zhao, H. Y. Li, D. X. Wang, *Inorg. Chem.* **2003**, *42*, 8446–8448.
- [71] M. F. Erben, R. M. Rosana, C. O. Della Védova, *J. Phys. Chem. A* **2004**, *108*, 3938–3946.
- [72] S. E. Ulic, C. O. Della Védova, A. Hermann, H.-G. Mack, H. Oberhammer, *Inorg. Chem.* **2002**, *41*, 5699–5705.
- [73] L. Du, L. Yao, X. Q. Zeng, M. F. Ge, D. X. Wang, *J. Phys. Chem. A* **2007**, *111*, 4944–4949.
- [74] X. J. Zhu, M. F. Ge, J. Wang, Z. Sun, D. X. Wang, *Angew. Chem. Int. Ed.* **2000**, *39*, 1940–1943.
- [75] M. J. Frisch, G. W. Trucks, H. B. Schlegel, G. E. Scuseria, M. A. Robb, J. R. Cheeseman, J. A. Montgomery Jr, T. Vreven, K. N. Kudin, J. C. Burant, J. M. Millam, S. S. Iyengar, J. Tomasi, V. Barone, B. Mennucci, M. Cossi, G. Scalmani, N. Rega, G. A. Petersson, H. Nakatsuji, M. Hada, M. Ehara, K. Toyota, R. Fukuda, J. Hasegawa, M. Ishida, T. Nakajima, Y. Honda, O. Kitao, H. Nakai, M. Klene, X. Li, J. E. Knox, H. P. Hratchian, J. B. Cross, C. Adamo, J. Jaramillo, R. Gomperts, R. E. Stratmann, O. Yazyev, A. J. Austin, R. Cammi, C. Pomelli, J. W. Ochterski, P. Y. Ayala, K. Morokuma, G. A. Voth, P. Salvador, J. J. Dannenberg, V. G. Zakrzewski, S. Dapprich, A. D. Daniels, M. C. Strain, Ö. Farkas, D. K. Malick, A. D. Rabuck, K. Raghavachari, J. B. Foresman, J. V. Ortiz, Q. Cui, A. G. Baboul, S. Clifford, J. Cioslowski, B. B. Stefanov, G. Liu, A. Liashenko, P. Piskorz, I. Komaromi, R. L. Martin, D. J. Fox, T. Keith, M. A. Al-Laham, C. Y. Peng, A. Nanayakkara, M. Challacombe, P. M. W. Gill, B. Johnson, W. Chen, M. W. Wong, C. Gonzalez, J. A. Pople, *Gaussian 03*, revision B.01, Gaussian, Inc., Pittsburgh PA, **2003**.

Received: April 30, 2008

Published Online: July 31, 2008